THEORETICAL AND NUMERICAL STUDY OF THE CONVERGENCE OF LUENBERGER OBSERVERS FOR A LINEARIZED WATER WAVE MODEL

PIERRE LISSY* AND LUCAS PERRIN†

Abstract. This paper investigates the convergence properties of Luenberger observers applied to a linearized water wave model. The study is motivated by the challenge of estimating wave dynamics when only partial free surface measurements are available. We identify fundamental obstructions to convergence, showing that the classical Luenberger observer fails to achieve full-state reconstruction due to challenges associated with mean-value modes and high-frequency components. To overcome these limitations, we introduce modified observer schemes that incorporate frequency filtering and projection techniques. Our theoretical results are reinforced by numerical experiments that demonstrate the practical effectiveness of these observer-based estimation methods for water waves.

Key words. Linearized water wave equation, Luenberger observer, numerical simulations.

AMS subject classifications. 76B15, 93B53, 93C20

1. Introduction.

The study of water waves has long been a cornerstone of fluid mechanics, with broad applications in oceanography, naval engineering, and coastal management. These wave dynamics are governed by the water wave equations (WWE), derived from the incompressible Euler equations, which describe the free surface's evolution and the underlying fluid's velocity potential. However, to simplify the complex non-linearity of these equations, the linearized water wave equations (LWWE) are often employed. These equations, while capturing essential physical properties, allow for more tractable analytical and numerical investigations. They form the basis for the observer convergence analysis explored in this paper.

Recent research in the literature on fluid mechanics engineering science has focused on estimation and control techniques for wave systems, particularly in scenarios where direct measurements of the full state of the system are unavailable or impractical [9, 7, 10]. Luenberger observers, initially designed for linear systems, have been adapted to a range of complex applications, including fluid dynamics. The primary objective of our paper is to examine from the mathematical point of view the convergence properties of Luenberger observers when applied to the linearized water wave model, with partial data from the free surface (data coming from the whole surface have been studied in [36]). Although the existing literature offers a variety of methods for controlling and stabilizing water waves, there is a gap regarding the rigorous convergence analysis of such observers in the context of the LWWE with partial observation of the water surface.

Several works have investigated control and stabilization methods for water waves. Gagnon et al. [14] presented a Fredholm-type backstepping transformation to achieve rapid stabilization of the so-called capillary-gravity linearized water waves model, using spectral properties and controllability assumptions. We also refer to the contribution of Alazard et al. [1], who provided insights into the stabilization of water waves using pressure disturbances applied to the free surface. Further contributions in the field of stabilization include Su et al. [33], who investigated the stabilization of small-amplitude water waves using boundary controls. Note that the problem studied

*CERMICS, Ecole des Ponts, IP Paris, Marne-la-Vallée, France (pierre.lissy@enpc.fr).
†Dep. Math. Stat., Univ. Konstanz, Konstanz, Germany (lucas.perrin@uni-konstanz.de).

in this paper has similarities to that of damped wave equations. We refer to [31] for a comprehensive review of this problem.

While previous studies have concentrated on stabilization and controllability for both linear and non-linear water wave models, our work provides a novel approach by focusing specifically on the convergence of Luenberger observers in a linearized setting. The contribution of this paper is twofold. First, we establish some obstructions for the convergence of Luenberger observers applied to the LWWE, together with sufficient conditions to recover some "partial" and quantitative convergence results, leveraging spectral methods and operator theory. Related works are [15, 4], where the authors also study Luenberger observers or back and forth nudging algorithms for infinite-dimensional linear systems that are not fully reconstructible, as in the present situation. However, the results given in these articles do not apply in our context. Second, we validate these theoretical results through numerical simulations, demonstrating the practical applicability of observer-based estimation in water-wave systems.

This paper is organized as follows. Section 2 introduces the linearized water wave model. Section 3 sets the functional setting for our analysis. Section 4 delves into the main non-convergence results (Proposition 4.1 and Proposition 4.3) for the most natural Luenberger observer if we consider initial conditions in the natural energy space, or in a space of initial conditions with zero mean value. Section 5 aims to understand how to restore some partial and quantitative convergence theorems by changing the Luenberger observer (Theorem 5.1 and Theorem 5.2). Lastly, section 6 validates the theoretical analysis through numerical experiments and discusses the broader implications for observer design in fluid systems.

2. The linearized water waves equation. This paper focuses on linearized water waves (LWWE) equations. These equations are derived from a master model, that of water waves (WWE), itself derived from the incompressible Euler equations. These derivations can be found in [11] or [23]. Our geometric setting is summarized in Figure 2.1. We place ourselves in a domain Ω that describes the body of our fluid:

$$\Omega = \left\{(x,y) \in \mathbb{R}^2 | -d \leq y \leq \eta(t,x)\right\}.$$

The two main functions of interest are: $\psi(t,x,y)$ the velocity potential, at points (x,y) and time t and $\eta(t,x)$, the free surface elevation at point x and time t. $-d$ is a flat bottom. As described in [11] or [23] for water waves with a horizontal bottom and as described in [6] if we add the periodicity, ψ is harmonic in space:

$$\Delta\psi(t,x,y) = 0, \quad (x,y) \in \Omega, \quad t \in [0,+\infty). \tag{2.1}$$

Moreover, ψ is subject to the following boundary conditions:

$$\begin{aligned} \partial_y\psi(t,x,y) &= 0, && \text{on } y=-d,\\ \partial_t\psi(t,x,y) &= -g\eta(t,x), && \text{on } y=0,\\ \partial_t\eta(t,x) &= \partial_y\psi(t,x,y), && \text{on } y=0,\\ \psi(t,x,y) &= \psi(x+L,y,t), && (t,x,y) \text{ in } [0,+\infty)\times\Omega. \end{aligned} \tag{2.2}$$

The first boundary condition is referred to as the *bottom boundary condition* (*BBC*), the second as the *dynamic free surface boundary condition* (*DFSBC*), the third as the *kinematic free surface boundary condition* (*KFSBC*), and the last as

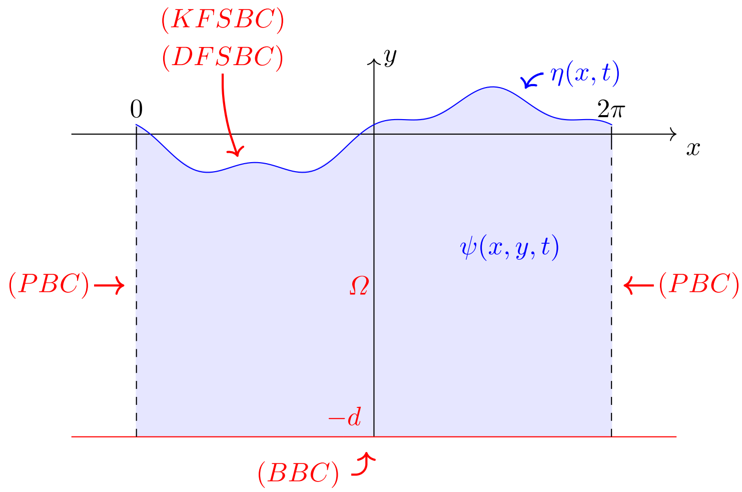

FIGURE 2.1. *Boundary problem for periodic water waves with flat bottom.*

the *periodic boundary condition* (*PBC*). Readers are again referred to [6], [23] or [11, Section 2.3] to see how the linearization around the rest state $y = 0$ of the Bernoulli equation leads to those conditions. Moreover, for computation simplification, we consider here x being on the torus $\mathbb{T} = \mathbb{R}/2\pi\mathbb{Z}$, *i.e.* choosing $L = 2\pi$. Under all these assumptions and after applying the boundary conditions, it is shown [11, 2.3] that the velocity potential $\psi(t, x, y)$ can be expressed simply at the surface as a function $\phi(t, x) = \psi(x, 0, t)$, and reconstructed throughout the whole domain Ω. This results in the following system of equations which is now on variables ϕ and η, respectively the velocity potential at the surface and the free surface displacement:

$$
\begin{cases}
\partial_t \phi(t, x) & = -g\eta(t, x), \\
\partial_t \eta(t, x) & = \mathcal{G}(\phi(t, x)),\ (t, x) \in [0, +\infty) \times \mathbb{T}, \\
\phi(0, x) = \phi^0(x), \quad \eta(0, x) & = \eta^0(x),
\end{cases}
\tag{2.3}
$$

where the operator $\mathcal{G}$ can be seen as a Dirichlet-to-Neumann map that does the link between the velocity potential throughout the whole domain ψ, and the velocity potential at the surface ϕ. This operator is such that $\mathcal{G} : \phi \mapsto \partial_y \psi(t, x, y)_y|_{y=0}$. Therefore, following [11, Section 2.3], the operator $\mathcal{G}$ is in Fourier space

$$
\mathcal{F}\left[\mathcal{G}(\phi)\right](n) = |n| \tanh(d|n|) \mathcal{F}\left[\phi\right](n),\ n \in \mathbb{Z}.
\tag{2.4}
$$

where $\mathcal{F}[\cdot]$ is the Fourier transform on $\mathbb{T}$. Due to (2.4), it is easy to obtain that functions of the form:

$$
(\phi, \eta)^t = (\phi_0 e^{i(nx - \omega_n t)}, \eta_0 e^{i(nx-\omega_n t)})^t
\tag{2.5}
$$

with ω_n the angular frequency, are solutions of (2.3), provided that

$$
i\omega_n \phi_0 = g\eta_0,
\tag{2.6}
$$

and the following (dispersion) relation holds:

$$
(\omega_n)^2 = g|n| \tanh(d|n|).
\tag{2.7}
$$

3. Functional setting. Let us give now some appropriate functional setting. Let us introduce the spaces

$$L^2_p = L^2(\mathbb{T}) = \left\{ f = \sum_{n\in\mathbb{Z}} f_n e^{inx} \text{ such that } ||f||^2_{L^2_p} := \sum_{n\in\mathbb{Z}} |f_n|^2 < +\infty \right\},$$

$$H^{1/2}_p = \left\{ f = \sum_{n\in\mathbb{Z}} f_n e^{inx} \in L^2_p \text{ such that } ||f||^2_{H^{1/2}_p} := |f_0|^2 + \sum_{n\in\mathbb{Z}^*} |n||f_n|^2 < +\infty \right\},$$

$$H^1_p = \left\{ f = \sum_{n\in\mathbb{Z}} f_n e^{inx} \in L^2_p \text{ such that } ||f||^2_{H^1_p} := |f_0|^2 + \sum_{n\in\mathbb{Z}^*} n^2|f_n|^2 < +\infty \right\}.$$

Each of these spaces is endowed with the scalar product naturally associated to the norm appearing in the definition. With these scalar products, they are Hilbert spaces. Remark that, notably, by the Plancherel Theorem,

$$||f||^2_{L^2_p} = \frac{1}{2\pi}\int_{\mathbb{T}} |f|^2, \ \forall f \in L^2_p. \tag{3.1}$$

Thanks to (2.4), the operator $\mathcal{G}$ can be expressed as follows:

$$\forall f = \sum_{n\in\mathbb{Z}} f_n e^{inx} \in H^1_p,\ \mathcal{G}f(x) = \sum_{n\in\mathbb{Z}^*} |n|\tanh(d|n|) f_n e^{inx} \left(\in L^2_p\right). \tag{3.2}$$

Now, consider the operator A defined as:

$$A := \begin{pmatrix} 0 & -gI \\ \mathcal{G} & 0 \end{pmatrix}, \tag{3.3}$$

with state space $H = H^{1/2}_p \times L^2_p$ and domain $D(A) = H^1_p \times H^{1/2}_p$, endowed respectively with the hilbertian norms (for which they are Hilbert spaces)

$$||(f,g)||^2_H = ||f||^2_{H^{1/2}_p} + ||g||^2_{L^2_p},\ ||(f,g)||^2_{D(A)} = ||f||^2_{H^1_p} + ||g||^2_{H^{1/2}_p}.$$

In this setting, the linearized water waves equations for periodic waves with an horizontal bottom given in (2.3) can be written as:

$$\begin{cases} \partial_t y(t,x) &= Ay(t,x), \\ y(0,x) &= y_0(x), \end{cases} (t,x) \in [0,+\infty) \times \mathbb{T}, \tag{3.4}$$

where $y = (\phi, \eta)^t$ and $y^0 = (\phi^0, \eta^0)^t$.

3.1. Spectral analysis of $\mathcal{G}$ and A. With the expression (3.2), it is easy to see that the distinct eigenvalues of the self-adjoint operator $\mathcal{G}$ are given by the eigenvalue 0 (associated to the constant eigenfunction 1), and by the eigenvalues $\mu_k = |k|\tanh(d|k|)$, $k \in \mathbb{N}^*$, which are of multiplicity 2, with the associated orthogonal basis of eigenfunctions given by e^{ikx} and e^{-ikx}.

Contrarily to many usual situations, let us emphasize that 0 is an eigenvalue of A, so that A is not a positive definite operator, but only a semi-definite operator. Hence, the usual theory to pass from first-order to second-order operators (see *e.g.* [34, Section 6.8]) cannot be applied, and notably, A is *not* a skew-adjoint operator.

This will be an additional difficulty, taking into account that many results in the literature of Luenberger observers (or stabilization) are restricted to this case (see notably various results in [24, 15, 4, 5]).

However, it is quite easy to discover that A is "almost" skew-adjoint and to derive an appropriate spectral decomposition. The distinct eigenvalues of A are given by the two families

$$\lambda_k^+ = i\sqrt{g\mu_k} = i\sqrt{gk\tanh(dk)},\ \lambda_k^- = -i\sqrt{g\mu_k} = -i\sqrt{gk\tanh(dk)},\ k \in \mathbb{N}^*,$$

each different eigenvalue being of algebraic and geometric multiplicity 2, together with the eigenvalue 0, which is of algebraic multiplicity 2 and geometric multiplicity 1 (which means that we have a generalized eigenfunction associated to the eigenvalue 0). For $|n| = k$ with $k \neq 0$, a basis of orthonormal eigenfunctions associated to the corresponding eigenspace is given by

$$\nu_n^+ = \frac{1}{\sqrt{2|n|g}}\begin{pmatrix} i\sqrt{g}e^{inx} \\ \sqrt{|n|}e^{inx}\end{pmatrix}, \quad \nu_n^- = \frac{1}{\sqrt{2|n|g}}\begin{pmatrix} -i\sqrt{g}e^{inx} \\ \sqrt{|n|}e^{inx}\end{pmatrix}. \tag{3.5}$$

A normalized eigenfunction associated to 0 is given by

$$\nu_0^+ = \frac{1}{\sqrt{2}}\begin{pmatrix} 1 \\ 0 \end{pmatrix}. \tag{3.6}$$

and an (orthogonal) generalized and normalized eigenfunction is given by

$$\nu_0^- = \frac{1}{\sqrt{2}}\begin{pmatrix} 0 \\ 1 \end{pmatrix}. \tag{3.7}$$

The family of usual and generalized eigenfunctions forms a Hilbert basis in L^2_p.

3.2. Well-posedness and conserved quantities. Let us introduce some additional notations, that will be useful for proving well-posedness of (2.3). We introduce

$$L^2_{p,0} = \left\{ f \in L^2_p \text{ such that } \int_{\mathbb{T}} f = 0 \right\} = \left\{ \sum_{n\in\mathbb{Z}} f_n e^{inx} \in L^2_p \text{ such that } f_0 = 0 \right\},$$

$$H^{1/2}_{p,0} = \left\{ f = \sum_{n\in\mathbb{Z}^*} f_n e^{inx} \in L^2_{p,0} \text{ such that } ||f||^2_{H^{1/2}_{p,0}} := \sum_{n\in\mathbb{Z}^*} |n||f_n|^2 < +\infty \right\},$$

$$H^1_{p,0} = \left\{ f = \sum_{n\in\mathbb{Z}} f_n e^{inx} \in L^2_{p,0} \text{ such that } ||f||^2_{H^1_{p,0}} := \sum_{n\in\mathbb{Z}^*} n^2 |f_n|^2 < +\infty \right\}.$$

These spaces are endowed with the natural scalar product and norms induced by their definitions, that we denote respectively by $||\cdot||_{L^2_{p,0}}, ||\cdot||_{H^{1/2}_{p,0}}, ||\cdot||_{H^1_{p,0}}$ (notice that we can extend these norms as semi-norms respectively on $L^2_p, H^{1/2}_p, H^1_p$, which corresponds to forgetting the mode 0, *i.e.* the mean, of the functions under study, and that these norms are nothing else than the restrictions of the norms $||\cdot||_{L^2_p}, ||\cdot||_{H^{1/2}_p}, ||\cdot||_{H^1_p}$ on $L^2_{p,0}$, $H^{1/2}_{p,0}$, $H^1_{p,0}$).

Following the proof of [36, Theorem 1], we obtain that A, with domain

$$\mathcal{D}_0(A) = H^1_{p,0} \times H^{1/2}_{p,0},$$

is the generator of a C^0-semigroup of operators on $H_0 := H^{1/2}_{p,0} \times L^2_{p,0}$ endowed with the natural scalar product, so that for any $(\phi^0, \eta^0) \in H_0$, there exists a unique solution $(\phi, \eta) \in C^0([0, +\infty), H_0)$ (We are exactly in the setting of [36], in this case). Moreover, it is easy to check that in the space H_0, $D_0(A^*) = D_0(A)$ and $A^* = -A$, so that A is in fact a generator of a C^0-group of operators on H_0.

Our next goal is now to understand how to obtain a well-posedness result on the whole state space H. This is the purpose of the following proposition.

Proposition 3.1. *A is the generator of a C^0-group of operators on H, so that for any $(\phi^0, \eta^0) \in H$, there exists a unique solution $(\phi, \eta) \in C^0([0, +\infty), H)$ to (2.3).*

Proof. We write $H^{1/2}_p \times L^2_p = H_0 \oplus_\perp E_0$, where H_0 is in fact the closure of the nonzero eigenspaces of A and E_0 is the generalized eigenspace associated to 0. Associated with this decomposition, we have a natural decomposition of $A = A_0 + A_1$, where

$$A_{0|H_0} = A,\ A_{0|E_0} = 0 \text{ and } A_{1|H_0} = 0,\ A_{1|E_0} = A.$$

Hence, by the previous discussion, it is clear that A_0 is the generator of a strongly continuous semigroup on H. Moreover, A_1 is clearly a bounded operator, since E_0 is a finite-dimensional space. We deduce (see *e.g.* [34, Theorem 2.11.2]) that A is indeed the generator of a C^0-semigroup of operators on H. Moreover, the same analysis applies if we replace A by $-A$ (because A_0 is skew-adjoint, so $-A_0$ is also the generator of a strongly continuous semigroup on H, and $-A_1$ is still bounded), so $-A$ is also the generator of a strongly continuous semigroup on H. We deduce by applying [34, Proposition 2.7.8] that A is the generator of a strongly continuous group on H. ∎

For a solution $y = (\phi, \eta)$ of (3.4), we introduce the following energy

$$E(y,t) = \frac{1}{2}\left(g\int_{\mathbb{T}} (\eta(t,x))^2 dx + \int_{\mathbb{T}} (\sqrt{\mathcal{G}}\phi(t,x))^2 dx\right). \tag{3.8}$$

Differentiating formally this expression, using (3.4), and the fact that $\mathcal{G}$ is selfadjoint, we deduce that

$$\begin{aligned}
\frac{d}{dt}E(y,t) &= g\int_{\mathbb{T}} \eta(t,x)\partial_t\eta(t,x)dx + \int_{\mathbb{T}} \sqrt{\mathcal{G}}\phi(t,x)\partial_t\left(\sqrt{\mathcal{G}}\phi\right)(t,x)dx \\
&= g\int_{\mathbb{T}} \eta(t,x)\mathcal{G}\phi(t,x)dx + \int_{\mathbb{T}} \sqrt{\mathcal{G}}\phi(t,x)\sqrt{\mathcal{G}}\left(\partial_t\phi\right)(t,x)dx \\
&= g\int_{\mathbb{T}} \eta(t,x)\mathcal{G}\phi(t,x)dx + \int_{\mathbb{T}} \mathcal{G}\phi(t,x)\left(\partial_t\phi\right)(t,x)dx \\
&= g\int_{\mathbb{T}} \eta(t,x)\mathcal{G}\phi(t,x)dx + \int_{\mathbb{T}} \mathcal{G}\phi(t,x)(-g\eta(t,x))dx \\
&= 0,
\end{aligned}$$

so that $E(y,t)$ is conserved:

$$E(y(t,x)) = \frac{1}{2}\left(g\int_{\mathbb{T}} (\eta^0)^2 + \int_{\mathbb{T}} (\mathcal{G}\phi^0)^2\right). \tag{3.9}$$

These computations can be made rigorous by taking initial conditions in $D(A)$ and using an easy density argument.

Let us give some invariant quantities that are inherent to (3.4). By the definition of $\mathcal{G}$ given in (3.2), for any $f \in H^{1/2}(\mathbb{T})$, we have $\int_{\mathbb{T}} \mathcal{G} f = 0$. Notably, using the second equation of (3.4) and integrating in space on $\mathbb{T}$, formally, any solution (ϕ, η) is such that

$$\partial_t \left(\int_{\mathbb{T}} \eta(t, \cdot) \right) = \int_{\mathbb{T}} \mathcal{G}\phi(t, \cdot) = 0,$$

so that $\int_{\mathbb{T}} \eta(t, \cdot)$ remains constant over time:

$$\forall t \geqslant 0, \int_{\mathbb{T}} \eta(t, \cdot) = \int_{\mathbb{T}} \eta^0. \tag{3.10}$$

Hence, the first equation of (3.4) integrated in space on $\mathbb{T}$ also gives that

$$\partial_t \left(\int_{\mathbb{T}} \phi(t, \cdot) \right) = -g \int_{\mathbb{T}} \eta^0,$$

so that

$$\forall t \geqslant 0, \int_{\mathbb{T}} \phi(t, \cdot) = \int_{\mathbb{T}} \phi^0 - gt \int_{\mathbb{T}} \eta^0. \tag{3.11}$$

These quantities are perfectly known as soon as the initial conditions are known. Conversely, knowing the mean value of ϕ and η at any time $t \geqslant 0$ is enough to recover the zero mode of η^0 and ϕ^0. Hence, if we assume that for some extra reason, we are able to reconstruct or guess what are the mean value of $\eta(t, \cdot)$ and $\phi(t, \cdot)$, then, it is possible to reconstruct the first mode of η^0 and ϕ^0. Here also, these computations can be made rigorous by taking initial conditions in $D(A)$ and using an easy density argument.

The core idea of this paper is that, unlike in [36], we place ourselves in a setting where we only get a partial measurement of the surface $\eta(t, x)$: $y(t, x) = \mathbf{1}_\omega(x)\eta(t, x)$, where ω is an open subset of $\mathbb{T}$ that is distinct from $\mathbb{T}$. However, contrarily to the result given in [36], this partial measurement is not enough to reconstruct the solution of (3.4), as it is proved later on, and we need to find another strategy to recover at least low frequencies different from 0. The first Luenberger-like observer we will study is the following natural one:

$$\begin{cases} \partial_t \hat{\phi}(t, x) &= -g\hat{\eta}(t, x), \\ \partial_t \hat{\eta}(t, x) &= \mathcal{G}\hat{\phi}(t, x) - \gamma \mathbf{1}_\omega(x)(\eta(t, x) - \hat{\eta}(t, x)), \\ \hat{\phi}(0, x) &= \hat{\phi}^0(x), \quad \hat{\eta}(0, x) = \hat{\eta}^0(x), \end{cases} \tag{3.12}$$

where $\gamma > 0$ the correction gain, and $(\hat{\phi}, \hat{\eta})^{\mathrm{T}}$ the observer trajectory of the state $(\phi, \eta)^{\mathrm{T}}$.

Then, $(\phi_{er}, \eta_{er}) := (\phi - \hat{\phi}, \eta - \hat{\eta})$ is solution to

$$\begin{cases} \partial_t \phi_{er}(t, x) &= -g\eta_{er}(t, x), \\ \partial_t \eta_{er}(t, x) &= \mathcal{G}\phi_{er}(t, x) - \gamma \left(\mathbf{1}_\omega(x)\eta_{er}(t, x) \right), \\ \phi_{er}(0, x) &= \phi^0_{er}(x), \quad \eta_{er}(0, x) = \eta^0_{er}(x), \end{cases} \tag{3.13}$$

where $\phi^0_{er}(x) = \phi^0(x) - \hat{\phi}^0(x)$ and $\eta^0_{er}(x) = \eta^0(x) - \hat{\eta}^0(x)$.

To conclude, let us introduce the control and feedback operators. We consider the control space U to be the same as the state space H. They are respectively given by

$$B = \begin{pmatrix} 0 & 0 \\ 0 & 1_\omega \end{pmatrix} \in \mathcal{L}_c(H) \text{ and } K = \gamma I_d \in \mathcal{L}_c(H), \tag{3.14}$$

so that (3.13) can be also abstractly written as

$$\begin{cases} \partial_t \begin{pmatrix} \phi_{er}(t,x) \\ \eta_{er}(t,x) \end{pmatrix} & = (A - BK) \begin{pmatrix} \phi_{er}(t,x) \\ \eta_{er}(t,x) \end{pmatrix}, \\ \begin{pmatrix} \phi_{er}(0,x) \\ \eta_{er}(0,x) \end{pmatrix} & = \begin{pmatrix} \phi^0_{er}(x) \\ \eta^0_{er}(x) \end{pmatrix}. \end{cases} \tag{3.15}$$

4. Non-reconstruction results for the localized Luenberger observer on the whole state space.

4.1. Obstruction coming from the mean value. Let us prove the following easy fact.

PROPOSITION 4.1. *(3.13) is not asymptotically stable: there exists $y_0 \in H$ such that the corresponding solution y to (3.13) does not verify $||y(t)||_H \to 0$ as $t \to +\infty$.*

Proof. This is just a question of remarking that ν_0^+ defined in (3.6) is still an eigenfunction of the operator $A - BK$, associated to the eigenvalue 0. Indeed, we have

$$(A - BK)\nu_0^+ = A\nu_0^+ - \gamma B \nu_0^+ = \begin{pmatrix} 0 \\ 0 \end{pmatrix}.$$

Hence, the corresponding solution to (3.13) is constant in time and given by

$$(\phi_{er}(t,x), \eta_{er}(t,x)) = \nu_0^+.$$

Hence, for such a solution, $||y(t)||_H$ is a non-zero constant and cannot go to 0 as $t \to +\infty$. ∎

According to Proposition 4.1, it is tempting to try to stabilize all frequencies except the 0 one, corresponding to the mean value.

4.2. Obstruction coming from the high frequencies for the original Luenberger observer. A key point in order to prove that the Luenberger observer does not converge exponentially even if we do not wish to reconstruct the mean value is the following result, which might be of independent interest.

LEMMA 4.2. *Let $\mathcal{H}$ and $\mathcal{U}$ be two Hilbert spaces. Assume that $\mathcal{A}$ is the generator of a C^0-group of operators on $\mathcal{H}$, and that $\mathcal{B} \in \mathcal{L}_c(\mathcal{U}, \mathcal{H})$. Assume that $\mathcal{P} \in \mathcal{L}_c(\mathcal{H})$ is a projection on the closed subspace $\mathcal{F} = \mathcal{P}(\mathcal{H})$, and that $\mathcal{P}$ commutes with $\mathcal{A}$. Let us introduce the growth bound of $-\mathcal{A}$, given by*

$$\omega_0(-\mathcal{A}) := \lim_{t \to +\infty} t^{-1} \log \left(||e^{-tA}|| \right). \tag{4.1}$$

Assume that there exists $\mathcal{K} \in \mathcal{L}_c(\mathcal{H}, \mathcal{U})$, $C > 0$ and $\lambda > \omega_0(-\mathcal{A})$ such that for any $y^0 \in \mathcal{F}$, the solution to the abstract linear feedback system

$$\begin{cases} y' & = \mathcal{A}y + \mathcal{B}\mathcal{K}y, \\ y(0) & = y^0 \end{cases} \tag{4.2}$$

verifies

$$\forall t \geqslant 0,\ ||\mathcal{P}y(t)||_H \leqslant Ce^{-\lambda t}||y^0||_H. \tag{4.3}$$

Then, there exists $T > 0$ such that for any $y^0 \in \mathcal{F}$, there exists $u \in L^2((0,T),\mathcal{U})$ such that the solution y to the control system

$$\begin{cases} y' &= \mathcal{A}y + \mathcal{B}u, \\ y(0) &= y^0 \end{cases} \tag{4.4}$$

verifies $\mathcal{P}(y(T)) = 0$.

Proof. Our proof is inspired by [24, Theorem 2.4]. Assume that (4.3) holds. Let $T > 0$ and

$$J(T) = \mathcal{P}e^{-T\mathcal{A}}e^{T(\mathcal{A}+\mathcal{B}\mathcal{K})} \in \mathcal{L}_c(\mathcal{F}), \tag{4.5}$$

Where $\mathcal{F}$ is endowed with the norm on $\mathcal{H}$. Moreover, since $\mathcal{P}$ commutes with $\mathcal{A}$,

$$||J(T)|| \leqslant ||e^{-T\mathcal{A}}||\, ||\mathcal{P}e^{T(\mathcal{A}+\mathcal{B}\mathcal{K})}||. \tag{4.6}$$

(4.3) gives that as an operator from $\mathcal{F}$ to $\mathcal{F}$ endowed with the norm of $\mathcal{H}$, we have

$$||\mathcal{P}e^{T(\mathcal{A}+\mathcal{B}\mathcal{K})}|| \leqslant Ce^{-\lambda T}.$$

Hence, the above inequality combined with (4.6) (remind that $\lambda > \omega_0(-\mathcal{A})$) ensures that $||J(T)|| < 1$ for T large enough. Hence, setting $J = J(T)$ for such a fixed T, we have that $I - J$ is invertible and $(I - J)^{-1} \in \mathcal{L}_c(\mathcal{F})$.

Now, let $y^0 \in \mathcal{F}$. For $t \in [0, T]$, we set

$$z_1(t) = e^{t(\mathcal{A}+\mathcal{B}\mathcal{K})}(I - J)^{-1}y_0 \in H,\ z_2(t) = e^{t\mathcal{A}}(I - (I - J)^{-1})y_0 \in H.$$

Seeing $(I - J)^{-1}y_0$ and $(I - (I - J)^{-1})y_0$ as elements of $\mathcal{H}$ and using a perturbation property of semigroups (see [28, Section 3.1, Formula (1.2)], we have

$$y(t) := z_1(t) + z_2(t) = e^{tA}y_0 + \int_0^t e^{(t-s)\mathcal{A}}\mathcal{B}\mathcal{K}z_1(s)ds. \tag{4.7}$$

Clearly, $y(0) = y^0$. Moreover, from the expression of J given in (4.5), together with the fact that $\mathcal{P}$ and $\mathcal{A}$ commute, we deduce that

$$Pe^{T(\mathcal{A}+\mathcal{B}\mathcal{K})} = e^{T\mathcal{A}}J.$$

Using that $y_0 \in \mathcal{F} = \mathcal{P}(\mathcal{H})$, that $\mathcal{P}$ and $\mathcal{A}$ commute, and that $\mathcal{P}$ is a projection on $\mathcal{F}$, (so that $\mathcal{P}((I - J)^{-1})y_0 = ((I - J)^{-1}y_0)$, we obtain

$$\begin{aligned} \mathcal{P}(y(T)) &= \mathcal{P}\left(e^{T(\mathcal{A}+\mathcal{B}\mathcal{K})}(I - J)^{-1}y_0\right) + \mathcal{P}\left(e^{TA}(I - (I - J)^{-1})y_0\right) \\ &= e^{T\mathcal{A}}\left(J(I - J)^{-1} + (I - (I - J)^{-1})\right)y_0 \\ &= 0, \end{aligned}$$

whence the result by taking as a control

$$u(t) = \mathcal{K}z_1(t) \in L^2((0,T),\mathcal{U}),$$ ∎

using (4.7) and the Duhamel formula.

Applying the previous proposition gives the following negative result.

PROPOSITION 4.3. (3.13) *is not exponentially stable with respect to the semi-norm* $||\cdot||_{H^{1/2}_{p,0}} \times ||\cdot||_{L^2_{p,0}}$.

Proof. We reason by contradiction. We assume that for any $(\phi^0_{er}, \eta^0_{er})$, the solution (ϕ_{er}, η_{er}) to (3.12) converges exponentially to 0 in the $||\cdot||_{H^{1/2}_{p,0}} \times ||\cdot||_{L^2_{p,0}}$ semi-norm as $t \to +\infty$.

We can apply Lemma 4.2 with $\mathcal{A} = A$ (which is of growth bound 0), $\mathcal{B} = B$, $\mathcal{K} = K$ and $\mathcal{P}$ is the orthogonal projection on $\mathcal{F} = H_0 = H^{1/2}_{p,0} \times L^2_{p,0}$, which commutes with A (see the beginning of the proof of Proposition 4.1). We deduce that there exists $T > 0$ for which for any $(\phi^0, \eta^0) \in H^{1/2}_{p,0} \times L^2_{p,0}$, there exists $v \in L^2((0,T), \mathbb{T})$ such that the solution (ϕ, η) to

$$\begin{cases} \partial_t \phi(t,x) & = -g\eta(t,x), \\ \partial_t \eta(t,x) & = \mathcal{G}\phi(t,x) + \mathbf{1}_\omega(x) v(t,x), \\ \phi(0,x) = \phi^0(x), \quad \eta(0,x) & = \eta^0(x), \end{cases} \tag{4.8}$$

is such that $\mathcal{P}(\phi(T,\cdot), \eta(T,\cdot)) = 0$. Since $\mathcal{F}^\perp = E_0$ (the generalized eigenspace associated to 0), this implies that both $\phi(T,\cdot)$ and $\eta(T,\cdot)$ are constants.

Now, we introduce

$$u = \frac{i}{\sqrt{g}} \sqrt{\mathcal{G}} \phi + \eta.$$

Then, using (4.8), u solves

$$\begin{cases} \partial_t u & = -i\sqrt{g}\sqrt{\mathcal{G}} u + \mathbf{1}_\omega v, \\ u(0,x) & = \frac{i}{\sqrt{g}} \sqrt{\mathcal{G}} \phi^0(x) + \eta^0(x) \in L^2_{p,0}(\mathbb{T}). \end{cases}$$

Clearly,

$$(\phi^0, \xi^0) \in H^{\frac{1}{2}}_{p,0} \times L^2_{p,0} \mapsto \frac{i}{\sqrt{g}} \sqrt{\mathcal{G}} \phi^0(x) + \eta^0(x) \in L^2_{p,0}(\mathbb{T})$$

is onto. We deduce that for any $u^0 \in L^2_{p,0}$, there exists

$$(\phi^0, \xi^0) \in H^{\frac{1}{2}}(\mathbb{T})_{p,0} \times L^2_{p,0}$$

such that

$$u^0(x) = \frac{i}{\sqrt{g}} \sqrt{\mathcal{G}} \phi^0(x) + \eta^0(x).$$

For such ϕ^0, ξ^0, there exists $v \in L^2((0,T) \times \mathbb{T})$ such that the solution (ϕ, η) to (4.8) is such that $\phi(T,\cdot)$ and $\phi(T,\cdot)$ are constants. Hence, posing u as above, we deduce that the solution u of

$$\begin{cases} \partial_t u & = -i\sqrt{g}\sqrt{\mathcal{G}} u + \mathbf{1}_\omega w, \\ u(0,x) & = u^0(x), \end{cases} \tag{4.9}$$

verifies that $u(T,\cdot)$ is a constant.

Let us prove that we are in the setting of [21, Proposition 27], that enables to recover (under certain conditions) a full controllability result from a "partial" one, of the form as set out above. Let us locally use the notations of this article, for the sake of clarity.

We set $H = L^2_p$, that is indeed a complex Hilbert space for the natural scalar product. We set $U = L^2_p$, $U_T = U = L^2((0,T), L^2_p)$. It verifies the "extension by 0 property": if $w \in U_T$, $a, b > 0$, then the function $\widetilde{w}$ defined by $\widetilde{w}(t) = 0$ for $0 < t < a$, $\widetilde{w}(t) = w(t-a)$ for $a < t < T+a$, and $\widetilde{w}(t) = 0$ for $T+a < t < T+a+b$ is in $L^2((0, T+a+b), L^2_p)$.

We also set $A = -i\sqrt{g}\sqrt{\mathcal{G}}$, which is an unbounded operator with domain $H_p^{\frac{1}{2}}$, $\mathcal{F} = \mathrm{span}(1)$ (which is finite-dimensional and stable by e^{tA}), $\mathcal{S} = L^2_{p,0} = \mathrm{span}(1)^{\perp}$[1] (which is closed and finite codimensional), and $B = \mathbf{1}_\omega$. We have just proved that for any $u^0 \in \mathcal{S}$, there exists $w \in U_T$ such that the solution u of (4.9) verifies that $u(T, \cdot) \in \mathcal{F}$.

Moreover, A is diagonalizable and its eigenfunctions are the family of the complex exponentials $\{e^{inx}\}_{n\in\mathbb{Z}}$, which is well-known to be a linearly independent family on any open subset of $\mathbb{T}$. Hence, since $B^* = \mathbf{1}_\omega$, we indeed have by [21, Remark 28] that for any for every finite linear combination of generalized eigenfunctions g_0 of A^*, we have $B^* e^{tA^*} g_0 = 0$ on $(0, \varepsilon)$ for any $\varepsilon > 0$ implies that $g_0 = 0$.

Hence, we can apply [21, Proposition 27] and obtain the null controllability of (4.8) on the whole state space $L^2_p(\mathbb{T})$ at any time $T' > T$.

However, this turns out to be false. Indeed, using the formalism of [20], we can write

$$i\sqrt{g}\sqrt{\mathcal{G}} = \rho\left(\sqrt{-\Delta}\right),$$

with

$$\rho(x) = i\sqrt{g}\sqrt{x\tanh(x)}.$$

Remark that ρ is holomorphic on $\mathbb{C}^*$ and continuous on $\mathbb{C}$, and that $\rho(z) = o(z)$ as $z \to \infty$. Then, we can apply [20, Theorem 1.4] to obtain that (4.9) is not controllable in $L^2_p(\mathbb{T})$, whence the desired result by contradiction. ∎

5. Modifying the state space and the Luenberger observer.

As we have seen, we cannot have exponential stability of (3.13) because of two obstructions, one coming from the mean values and one coming from the high frequencies. Let us give two remedies to these problems.

5.1. State space of initial conditions with null mean value: polynomial decay.

Let us restrict our state space to the set of initial conditions with null mean values, *i.e.* we take as a state space H_0. Remark that it is not very convenient to look at (3.12) with initial state H_0. Indeed, if we are looking at (3.13), we observe that H_0 is not stable by the semigroup generated by the operator appearing in (3.13): if we start with initial conditions in H_0, then, in general, the term $\mathbf{1}_\omega \eta_{er}$ do not have mean value zero. One natural remedy is to "force" in some sense this property by projecting again on H_0. We call Π_{H_0} the orthogonal projection in H on the closed subspace H_0. According to the previous discussion, we first propose a new Luenberger observer leading to the system

$$(5.1)\qquad \begin{cases} \partial_t \hat{\phi}(t,x) &= -g\hat{\eta}(t,x), \\ \partial_t \hat{\eta}(t,x) &= \mathcal{G}\hat{\phi}(t,x) - \gamma \Pi_{H_0} \mathbf{1}_\omega(x)(\eta(t,x) - \hat{\eta}(t,x)), \\ \hat{\phi}(0,x) &= \hat{\phi}^0(x), \quad \hat{\eta}(0,x) = \hat{\eta}^0(x), \end{cases}$$

[1] We modified the notation $\mathcal{G}$ in [21, Proposition 27] into $\mathcal{S}$, to avoid confusions with the operator $\mathcal{G}$

where $(\hat{\phi}^0(x), \hat{\eta}^0(x)) \in H_0$. If $(\phi^0(x), \eta^0(x)) \in H_0$ and (ϕ, η) is the corresponding solution to (3.4), then, $(\phi_{er}, \eta_{er}) := (\phi - \hat{\phi}, \eta - \hat{\eta})$ is solution to

$$(5.2) \qquad \begin{cases} \partial_t \phi_{er}(t,x) & = -g\eta_{er}(t,x), \\ \partial_t \eta_{er}(t,x) & = \mathcal{G}\phi_{er}(t,x) - \gamma \Pi_{H_0}\left(\mathbf{1}_\omega(x)\eta_{er}(t,x)\right), \\ \phi_{er}(0,x) & = \phi^0_{er}(x), \quad \eta_{er}(0,x) = \eta^0_{er}(x), \end{cases}$$

where $\phi^0_{er}(x) = \phi^0(x) - \hat{\phi}^0(x)$ and $\eta^0_{er}(x) = \eta^0(x) - \hat{\eta}^0(x)$ are in H_0. For later purpose, we need to put our the control under the form of a collocated control. An explicit computations shows that $\gamma\Pi_{H_0}\mathbf{1}_\omega$ is a selfadjoint and non-negative operator on H_0. Hence, by functional calculus, it admits a unique square root denoted by $\tilde{B} = \sqrt{\gamma \Pi_{H_0}\mathbf{1}_\omega}$, which is also selfadjoint. Hence, this system can be rewritten in an abstract way as

$$(5.3) \qquad \begin{cases} \partial_t \begin{pmatrix} \phi_{er}(t,x) \\ \eta_{er}(t,x) \end{pmatrix} & = (\mathcal{A} - \tilde{B}\tilde{B}^*) \begin{pmatrix} \phi_{er}(t,x) \\ \eta_{er}(t,x) \end{pmatrix}, \\ \begin{pmatrix} \phi_{er}(0,x) \\ \eta_{er}(0,x) \end{pmatrix} & = \begin{pmatrix} \phi^0_{er}(x) \\ \eta^0_{er}(x) \end{pmatrix}. \end{cases}$$

Moreover, remind that we already remarked that $\mathcal{A}$ is the generator of a C^0-group on H_0 and that on H_0, $\mathcal{A}$ is skew-adjoint. Here, the high frequencies are still a problem, as shown in the next Proposition.

PROPOSITION 5.1. *(5.3) is not exponentially stable with respect to the* $||\cdot||_{H^{1/2}_{p,0}} \times ||\cdot||_{L^2_{p,0}}$*-norm.*

Proof. The proof is similar to the one of Proposition 4.3, but a little bit simpler. We reason by contradiction and we assume that (5.3) is exponentially stable. Since A is now skew-adjoint on H_0, one can apply [24, Theorem 2.3] (by seeing $\tilde{B}\tilde{B}^* = \Pi_{H_0}\mathbf{1}_\omega$ as a control and Id as a feedback operator) and deduce that (5.3) is exactly controllable at some time $T > 0$. Following the proof of Proposition 4.3, we reason by contradiction and we obtain that

$$(5.4) \qquad \begin{cases} \partial_t u & = -i\sqrt{g}\sqrt{\mathcal{G}}u + \mathbf{1}_\omega v, \\ u(0,x) & = u^0(x) \end{cases}$$

is null controllable in the state space $L^2_{p,0}$ at some time $T > 0$. By duality (see *e.g.*[Theorem 11.2.1]TW), this means that there exists $C > 0$ such that for any $\varphi^0 \in L^2_{p,0}$, we have

$$(5.5) \qquad ||\varphi(T,\cdot)||^2_{L^2} \leqslant \int_0^T \int_\omega |\varphi(t,x)|^2 dx dt,$$

where φ is the solution of the adjoint problem

$$\begin{cases} \partial_t \varphi & = -i\sqrt{g}\sqrt{\mathcal{G}}\varphi, \\ \varphi(0,x) & = \varphi^0(x). \end{cases}$$

It turns out that (5.5) is false. Indeed, the counterexample provided in [20, Proof of Theorem 1.4, Page 3145] is the periodization of a family of functions $(g_h)_{h\in(0,1)}$, defined on $\mathbb{R}$, that are compactly supported in the Fourier variable, with support away from $\xi = 0$. Notably, all the g_h are of mean 0 and are in L^2_p, so they lie in $L^2_{p,0}$ and furnish a counterexample for (5.5). ☐

However, even if one cannot expect exponential stabilization, we still have the following result.

THEOREM 5.1. *(5.3) is asymptotically stable with respect to the* $||\cdot||_{H^{1/2}_{p,0}} \times ||\cdot||_{L^2_{p,0}}$*-norm, in the sense that the solution of (5.3) converges strongly to 0 as* $t \to +\infty$*. Moreover, (5.3) enjoys the following polynomial decay: there exists* $C > 0$ *such that for any* $(\phi^0_{er}, \eta^0_{er}) \in D_0(A)$*, the corresponding solution of (5.3) verifies*

$$||(\phi_{er}(t,\cdot), \eta_{er}(t,\cdot))||_{H_0} \leqslant \frac{C}{\sqrt{1+t}} ||(\phi^0_{er}, \eta^0_{er})||_{D_0(A)},\ t \geqslant 0. \tag{5.6}$$

REMARK 5.2. *Remind that (5.6) cannot hold if we replace* $||(\phi^0_{er}, \eta^0_{er})||_{D_0(A)}$ *by* $||(\phi^0_{er}, \eta^0_{er})||_{H_0}$ *in the right-hand side, because of [13, Proposition V.1.7] (which asserts that in this case, (5.3) would be exponentially stable).*

Proof. We would like to prove that [32, Theorem 3.6] applies. Here, $A^* = -A$ has compact resolvents, and the feedback is under the form $-\tilde{B}\tilde{B}^*$ (see (5.3)), which is exactly the form of the feedback constructed in [32, Theorem 3.6] (since it relies on [32, Theorems 3.3, 3.4, 3.5]). Moreover, what is called "complete controllability" in [32] is exactly what is called *approximate observability in infinite time* in [34, Definition 6.5.1]. Applying [34, Proposition 6.9.1], we deduce that approximate observability in infinite time holds as soon as the Fattorini-Hautus test holds: there does not exists any eigenfunction φ of the operator $\mathcal{A}^*$ such that $\tilde{B}^*\varphi = 0$, which is equivalent to $\tilde{B}\tilde{B}^*\varphi = 0$. Reason by contradiction. For such an eigenfunction $\varphi(x) = \begin{pmatrix} \phi(x) \\ \eta(x) \end{pmatrix}$ of $A^* = -A$ associated to an eigenvalue $\lambda \neq 0$, $\tilde{B}^*\varphi = 0$ is therefore equivalent to: for every $x \in \omega$, we have $\eta(x) = 0$. In view of the eigenfunctions given in (3.5), η is a linear combination of a at most two distinct complex exponentials, that are well-known to form a linearly independent family on any interval (and so on ω), we deduce that $\eta(x) = 0$, $\forall x \in \mathbb{T}$. In view of the expression of $\mathcal{A}$, the fact that $\mathcal{A}\varphi = \lambda\varphi$ notably gives (by looking at the first component) that $-g\eta = \lambda\phi$. Since $\lambda \neq 0$, we also obtain that $\phi(x) = 0, \forall x \in \mathbb{T}$, which concludes the proof of the asymptotic stabilisation result by applying [32, Theorem 3.6].

Let us now explain how to prove (5.6). Our idea is to apply [5, Theorem 3.9]. In order to apply this Theorem, our first goal is to estimate

$$s||\tilde{D}^*((1+is)^2 + \mathcal{G}_{-1})^{-1}\tilde{D}||,\ s \in \mathbb{R}^+,$$

where $\tilde{D} = \tilde{D}^* = \sqrt{\gamma \Pi_{H_0} 1_\omega}$, and $\mathcal{G}_{-1}$ is the extension of $\mathcal{G}$ in $\mathcal{L}_c(H_0, D_0(A)')$. Remark that by [5, Section 2B], we have that for $s \geqslant 0$,

$$(s\tilde{D}^*((1+is)^2 + \mathcal{G}_{-1})^{-1}\tilde{D}) = \tilde{B}^*((1+is) - A_{-1})^{-1}\tilde{B}, \tag{5.7}$$

where A_{-1} is the extension of A in $\mathcal{L}_c(L^2_{p,0}, (H^1_{p,0})')$. Since $\tilde{B}^*$ is bounded, we have, for any $s \geqslant 0$,

$$||\tilde{B}^*((1+is) - A_{-1})^{-1}\tilde{B}|| \leqslant ||\tilde{B}^*||\,||((1+is) - A_{-1})^{-1}||\,||\tilde{B}||. \tag{5.8}$$

Since A has purely imaginary spectrum, we have the existence of $C > 0$ such that for any $s \geqslant 0$,

$$||\tilde{B}^*((1+is) - \mathcal{A}_{-1})^{-1}\tilde{B}|| \leqslant C.$$

Hence,coming back to (5.7), we have existence of some constant $C > 0$ such that for any $s \geqslant 0$, we have

$$s||\tilde{D}^*((1+is)^2 + \mathcal{G}_{-1})^{-1}\tilde{D}|| \leqslant C. \tag{5.9}$$

Moreover, the eigenvalues $\sqrt{\mu_k}$ of $\sqrt{\mathcal{G}}$ behave asymptotically as $C\sqrt{k}$ as $k \to +\infty$ for some $C > 0$. Notably, there exists $C > 0$ small enough such that for any $k \in \mathbb{N}^*$, we have

$$\sqrt{\mu_{k+1}} - \sqrt{\mu_k} \geqslant \frac{c}{\sqrt{\mu_k}}.$$

For $s \geqslant 0$, we set

$$\delta_0(s) = \frac{c}{4s}. \tag{5.10}$$

Then, for any $s \geqslant 0$, the set $[s - \delta_0(s), s + \delta_0(s)]$ contains at most one eigenvalue. We call $WP(s)$ the "wavepacket" associated to $s \geqslant 0$, *i.e.* the spectral subspace associated to the set $[s - \delta_0(s), s + \delta_0(s)]$, which is either empty, or limited to an eigenspace of a unique eigenvalue.

Consider any eigenfunction f of $\sqrt{\mathcal{G}}$ associated to an eigenvalue $\sqrt{\mu}_k$. Then, f can be written as $f(x) = a_k e^{ikx} + b_k e^{-ikx}$ with $a_k, b_k \in \mathbb{C}$. Moreover, writing $\omega = (\alpha, \beta)$ with $\alpha < \beta$, using $\Pi_{H_0} f = f$, the fact the scalar product on $L^2_{p,0}$ is the restriction of the scalar product on L^2_p, and (3.1),

$$\begin{aligned}
||\tilde{D}^* f||^2_{L^2_{p,0}} &= \langle \tilde{D}^* f, \tilde{D}^* f\rangle_{L^2_{p,0}} \\
&= \langle \tilde{D}\tilde{D}^* f, f\rangle_{L^2_{p,0}} \\
&= \langle \Pi_{H_0} \mathbf{1}_\omega f, f\rangle_{L^2_p} \\
&= \langle \mathbf{1}_\omega f, \Pi_{H_0} f\rangle_{L^2_p} \\
&= \langle \mathbf{1}_\omega f, f\rangle_{L^2_p} \\
&= \frac{1}{2\pi}\int_\omega |f|^2 \\
&= \frac{1}{2\pi}\int_\alpha^\beta \left(|a|^2 + |b|^2 + 2\mathrm{Re}(a\bar{b}e^{2ikx}\right) dx \\
&= \frac{\beta - \alpha}{2\pi}(|a|^2 + |b|^2) + \frac{1}{2\pi}\mathrm{Re}\left(a\bar{b}\int_\alpha^\beta e^{2ikx} dx\right) \\
&= \frac{\beta - \alpha}{2\pi}(|a|^2 + |b|^2) + \mathrm{Re}\left(a\bar{b}\frac{e^{2ik\beta} - e^{2ik\alpha}}{\pi i k}\right).
\end{aligned}$$

Since $\int_{\mathbb{T}} |f|^2 = |a|^2 + |b|^2$, we deduce that as soon as $f \neq 0$, we have $||\tilde{D}^* f||^2_{L^2_{p,0}} \neq 0$ and, by Young's inequality,

$$\frac{||\tilde{D}^* f||^2_{L^2_{p,0}}}{\int_{\mathbb{T}} |f|^2} \geqslant \frac{\beta - \alpha}{2\pi} - \frac{1}{\pi k} \to \frac{\beta - \alpha}{2\pi} > 0 \text{ as } |k| \to +\infty.$$

Hence, for some $C > 0$ small enough, we have have that

$$||\tilde{B}^* f||_{L^2_{p,0}} \geqslant C||f||_{L^2_{p,0}},\ f \in WP(s),\ s \geqslant 0. \tag{5.11}$$

Combining (5.9), (5.10) and (5.11), and applying [5, Theorem 3.9] gives that for some new $C > 0$

$$||(isId - (A - \tilde{B}\tilde{B}^*))^{-1}|| \leqslant Cs^2, \ s \in \mathbb{R}.$$

Applying [3, Theorem 2.4] gives that (for the operator norm in H_0)

$$(5.12) \qquad ||e^{t(A-\tilde{B}\tilde{B}^*)}(A - \tilde{B}\tilde{B}^*)^{-1}|| = O\left(\frac{1}{\sqrt{t}}\right), \ t \to +\infty.$$

We easily deduce (5.6) by applying this estimate together with the identity: $\forall \varphi \in D_0(A)$,

$$e^{t(A-\tilde{B}\tilde{B}^*)}\varphi = e^{t(A-\tilde{B}\tilde{B}^*)}(A - \tilde{B}\tilde{B}^*)^{-1}(A - \tilde{B}\tilde{B}^*)\varphi$$

and remarking that using a triangular inequality,

$$||(A - \tilde{B}\tilde{B}^*)\varphi|| \leqslant C||\varphi||_{D_0(A)}.$$

□

5.2. State space of low-frequency initial conditions with null mean value: exponential observer. A remedy is to look only at low-frequency functions. Let us fix some $N \in \mathbb{N}^*$. We call H^N the finite-dimensional space

$$H^N = \text{span}\{\nu_n^+, \nu_n^-\}_{1 \leqslant |n| \leqslant N}.$$

We also introduce $\Pi^N_{LF0^\perp}$ the orthogonal projection on H^N in H. We restrict ourselves to initial conditions in H^N and we propose the following observer:

(5.13)
$$\begin{cases} \partial_t \hat{\phi}(t,x) &= -g\hat{\eta}(t,x), \\ \partial_t \hat{\eta(t,x)} &= \mathcal{G}(\hat{\phi}(t,x)) - \gamma \Pi^N_{LF0^\perp} \mathbf{1}_\omega \left(\hat{\eta}(t,x) - \eta(t,x)\right), \, (t,x) \in [0,+\infty) \times \mathbb{T}, \\ \hat{\phi}(0,x) &= \hat{\phi}^0(x), \quad \hat{\eta}(0,x) = \hat{\eta}^0(x), \end{cases}$$

resulting in the error equation:

$$(5.14) \qquad \begin{cases} \partial_t \phi_{er}(t,x) &= -g\eta_{er}(t,x), \\ \partial_t \eta_{er}(t,x) &= \mathcal{G}(\phi_{er}(t,x)) - \Pi^N_{LF0^\perp} \mathbf{1}_\omega \eta_{er}(t,x), \, (t,x) \in [0,+\infty) \times \mathbb{T}, \\ \phi_{er}(0,x) &= \phi^0_{er}(x), \quad \eta_{er}(0,x) = \eta^0_{er}(x), \end{cases}$$

where $\phi^0_{er}(x) = \phi^0(x) - \hat{\phi}^0(x)$ and $\eta^0_{er}(x) = \eta^0(x) - \hat{\eta}^0(x)$. We then have the following result.

THEOREM 5.2. *(5.14) is exponentially stable, and there exists $C > 0$, independent of N, such that for any $(\phi^0_{er}(x), \eta^0_{er}(x)) \in H^N$ and any $t \geqslant 0$, we have*

$$(5.15) \qquad ||(\phi_{er}(t,\cdot), \eta_{er}(t,\cdot))||_{H_0} \leqslant C||(\phi^0_{er}(x), \eta^0_{er}(x))||_{H_0} e^{-\frac{C}{N}t}.$$

Proof. Introduce

$$B_N = \begin{pmatrix} 0 & 0 \\ 0 & \Pi^N_{LF0^\perp} 1_\omega \end{pmatrix}$$

and

$$\tilde{B}_N = \begin{pmatrix} 0 & 0 \\ 0 & \sqrt{\Pi^N_{LF0^\perp} 1_\omega} \end{pmatrix}.$$

Remark that $||\tilde{B}_N|| \leqslant C$, with C independent of N. Following the proof of Theorem 5.1, we deduce by using a similar estimate to (5.8) that we have an estimate similar to (5.9), namely,

$$s||\tilde{D}_N^*((1+is)^2+\mathcal{G}_{-1})^{-1}\tilde{D}_N|| \leqslant C,$$

where $\tilde{D}_N = \sqrt{\mathit{\Pi}^N_{LF0^\perp} 1_\omega}$ and $C>0$ is independent of N. Moreover, following exactly the notations and reasoning of the proof of Theorem 5.1, we also have the analogous of (5.11)

$$||\tilde{D}_N f||_{L^2_{p,0}} \geqslant C||f||_{L^2_{p,0}},\ f \in WP(s),\ s \geqslant 0,$$

where $C>0$ is independent of N and the wavepacket is defined with the same δ_0 as in (5.10). We deduce that a result similar to to (5.12), namely, for $t \geqslant C_1$ for some $C_1>0$ large enough, we have, for some $C>0$ independent of N.

$$(5.16) \qquad ||e^{t(A-B_N)}(A-B_N)^{-1}\varphi||_H \leqslant \frac{C||\varphi||_H}{\sqrt{t}},\ \forall \varphi \in H_N.$$

Assume now that φ is an eigenvector of $A-B_N$ associated to an eigenvalue $\lambda \in \mathbb{C}$. Such an eigenvalue is necessarily such that $\mathrm{Re}(\lambda)<0$.

Then, (5.16) becomes

$$\frac{e^{t\mathrm{Re}(\lambda)}}{|\lambda|}||\varphi||_H \leqslant \frac{C||\varphi||_H}{\sqrt{t}},\ t \geqslant C_1.$$

By an usual comparison principle, since the eigenvalue $\lambda_k^\pm$ of A behaves asymptotically as $\sqrt{|k|}$ as $|k| \to +\infty$ and since here $|k| \leqslant N$, we necessarily have that for some $C>0$,

$$|\lambda| \leqslant C\sqrt{N}.$$

We deduce that for some new $C>0$ and $t \geqslant C_1$,

$$e^{t\mathrm{Re}(\lambda)} \leqslant \frac{C\sqrt{N}}{\sqrt{t}}.$$

Now, we have two possibilities:

- Either $-\mathrm{Re}(\lambda) \geqslant 1/C_1$ (remind that $\mathrm{Re}(\lambda)<0$).
- Or $-\mathrm{Re}(\lambda) < 1/C_1$. In this case, taking $t=-1/\mathrm{Re}(\lambda) \geqslant C_1$, we deduce that

$$e^{-1} \leqslant C\sqrt{-N\mathrm{Re}(\lambda)}.$$

Hence, in this case, for some new $C>0$,

$$-\mathrm{Re}(\lambda) \geqslant \frac{C}{N}.$$

In both cases, for N large enough, we deduce that

$$\mathrm{Re}(\lambda) \leqslant -\frac{C}{N}.$$

Since λ can be any eigenvalue of $A-B_N$, an usual reasoning enables to deduce our desired result (5.15). $\square$

6. Numerical Results. This section is structured into four parts. The first part addresses certain numerical aspects that are worth discussing before proceeding with numerical experiments. Specifically, it covers the distinction between performing computations in Fourier space versus classical space, the interpretation of low-frequency projectors, and the phenomenon of aliasing. The second part focuses on validating the theoretical results presented earlier through numerical simulations. The third part explores the behavior of the convergence rate as a function of the number of available frequencies. Finally, the fourth part shifts to an application beyond the theoretical framework. Here, we apply a Luenberger observer to the problem of wave field reconstruction in open water. Data assimilation for wave fields is a crucial topic in addressing certain challenges in engineering and hydrodynamics. This research area has gained significant attention in recent years, with applications ranging from flood or tsunami prediction [30, 26] and bathymetry detection [18, 2] to the reconstruction and prediction of wave fields from observations [35, 12, 27, 22, 8]. Our last case focuses on the latter, making simplified assumptions while ensuring that the proposed method remains both relevant and practical. The approach is deliberately straightforward and easy to implement.

6.1. Numerical aspects. In this section, we clarify some numerical aspects that are important to address in the following section.

6.1.1. Fourier space and classical space. Let us first address the choice of the space (Fourier or classical) in which the numerical tests will be carried out. Computations for subsection 6.2 and subsection 6.3 are done in Fourier space. Computations for subsection 6.4 are performed in the classical space.

Concerning subsection 6.2 and subsection 6.3, this choice is motivated by the will to better represent the theoretical convergence results that we want to illustrate and to facilitate computations. But let us address the difference between running the simulations in a Fourier space and in classical space. Recall that for a periodic continuous function f on the torus $\mathbb{T}$, there exists an equivalence between the representation of the function on the grid $(f(x_i))_{i=\{0,\dots,N_x-1\}}$ and its representation in the Fourier domain $\mathcal{F}[f](n)_{n=\{-N_f,\dots,N_f\}}$ if $N_f=(N_x-1)/2$. This equivalence can be reworked with a simple discrete Fourier transform computation. However, this equivalence is no longer valid for piecewise continuous functions, which is our case because of the operator $\mathbf{1}_\omega$. In this setting we therefore lose the uniform and absolute convergence, but we still have convergence in L^2-norm, and almost everywhere convergence of the Fourier series to the function in the classical space thanks to classical theorems of Fourier analysis. It can be shown that the operators constructed thereafter in a discretized Fourier space converge towards the same operators constructed in a discretized classical space as N_x (or N_f) tends to infinity. The indicator operator $\mathbf{1}_\omega$ is then passed into Fourier space, assuming $\omega=[\pi-a,\pi+a]$, with:

$$c_0(\mathbf{1}_{[\pi-a,\pi+a]})=\frac{1}{2\pi}\int_0^{2\pi}\mathbf{1}_{[\pi-a,\pi+a]}(x)dx=\frac{a}{\pi} \tag{6.1}$$

and, for $n\in\mathbb{Z}\setminus\{0\}$,

$$c_n(\mathbf{1}_{[\pi-a,\pi+a]})=\frac{1}{2\pi}\int_0^{2\pi}\mathbf{1}_{[\pi-a,\pi+a]}(x)\exp(-inx)dx=\frac{a(-1)^n}{\pi}\frac{\sin(na)}{na}. \tag{6.2}$$

Regarding subsection 6.4, computations are carried out in the classical space as we approach a realistic and practical problem.

6.1.2. Projectors. Let us we clarify what *low-frequency projection* means in a numerical setting. Indeed, from the moment we carry out a discretization (Fourier or classical), this already amounts to carrying out a low-frequency projection of our continuous problem into a finite dimension setting since a discretization of our function can only represent a finite number of frequencies.

This is what is considered in the numerical test performed in subsection 6.4. The *low-frequency projection* is not visible in the formulations, but rather implied by the fact that we work in a discretized setting.

Regarding the first numerical test in subsection 6.2, as our aim is there to support the theoretical assertions made in this paper, *low-frequency projection* is defined as the operator that projects the solution onto the frequencies subspace that is the one of the initial condition. For example, if the initial condition of our initial value problem contains two sines of frequencies 1 and 2 (*i.e.*, $\sin(x) + \sin(2x)$), then the *low-frequency projection* operator projects a function in Fourier space onto frequencies $\{-2, -1, 0, 1, 2\}$. This initial condition is considered to be *low-frequency*.

6.1.3. Aliasing. One of the other numerical aspects that is important to specify is aliasing [25]. It is also known as spectral folding and occurs when we try to represent a function which contains more frequencies than the discretization grid can allow. The frequencies that are too high for the grid are then folded onto the rest of the frequencies, hence introducing a numerical error that cannot be avoided.

In order to avoid aliasing in subsection 6.2, we choose to concentrate on an initial condition that can be represented on the chosen frequency space. These are therefore sums of sines and cosines, which contain fewer frequencies than the frequency space can represent.

In subsection 6.4, this phenomenon is present as we aim to apply our observer on a more realistic setting. We are then outside the theoretical frame exposed above.

6.2. Numerical convergence of the error equation in the theoretical setting. In this section, we validate numerically the theoretical results presented above. Computations are performed in *MATLAB* [17]. We choose to emulate a discretization in space of the 1D torus $[0, 2\pi[$ with N_x points, *i.e.* a $\{x_0, x_1, \dots, x_{N_x-1}\}$ grid with $x_i = i\Delta x$, where $\Delta x = 2\pi/N_x$. For simplicity, we assume N_x to be odd, so that the maximum number of frequencies that can be represented with this discretization is $N_f = (N_x - 1)/2$. We therefore suppose to use a grid with $N_x = 2^6 + 1$ equidistant points, equivalent to the same number of frequencies, ranging from $-N_f = (N_x - 1)/2$ to $N_f = (N_x - 1)/2$. Computation are actually carried out in this frequency space.

We want to compare the results of different ODEs that describe the behaviour of the error without modifications (6.3), the error with a projector that removes the mean (6.4), and the error with a projector that removes the mean and high frequencies (6.5).

$$[\mathrm{E}_1] \Leftrightarrow \begin{cases} \partial_t \phi_{er}(t,x) = -g\eta_{er}(t,x) \\ \partial_t \eta_{er}(t,x) = \mathcal{G}(\phi_{er}(t,x)) - \mathbf{1}_\omega \eta_{er}(t,x) \end{cases} \tag{6.3}$$

$$[\mathrm{E}_2] \Leftrightarrow \begin{cases} \partial_t \phi_{er}(t,x) = -g\eta_{er}(t,x) \\ \partial_t \eta_{er}(t,x) = \mathcal{G}(\phi_{er}(t,x)) - \Pi_{\perp 0}\mathbf{1}_\omega \eta_{er}(t,x), \end{cases} \tag{6.4}$$

$$[\mathrm{E}_3] \Leftrightarrow \begin{cases} \partial_t \phi_{er}(t,x) = -g\eta_{er}(t,x) \\ \partial_t \eta_{er}(t,x) = \mathcal{G}(\phi_{er}(t,x)) - \Pi_{\perp 0}\Pi_{LF}\mathbf{1}_\omega \eta_{er}(t,x). \end{cases} \tag{6.5}$$

Here ω is defined as the interval $[\pi/2, 3\pi/2]$, representing an observation of half of the free surface.

Regarding the initial condition, remember that ϕ^0 and η^0 must satisfy relation (2.6), i.e., $\mathcal{F}\left[\eta^0\right](n) = \frac{i\omega_n}{g}\mathcal{F}\left[\phi^0\right](n)$ where $\mathcal{F}\left[\cdot\right]$ is the Fourier transform on $\mathbb{T}$. Same holds for $\hat{\eta}^0$ and $\hat{\phi}^0$ and consequently, for ϕ^0_{er} and η^0_{er}. We therefore choose to define ϕ^0_{er} as a signal with no mean defined as a sum of $N_{init} = 4$ sines and cosines:

$$\phi^0_{er}(x) = \sum_{n=1}^{n=N_{init}=4} \beta_{n,1}\sin(nx) + \beta_{n,2}\cos(nx), \tag{6.6}$$

with $\beta_{n,1}$ and $\beta_{n,2}$ taken at random from $[0,1]$ for each mode. Once ϕ^0_{er} is set, we choose η^0_{er} so that it follows relation (2.6) on each Fourier mode.

We discretize the operators associated with the dynamics of equations (6.3), (6.4) and (6.5) into matrices $\mathbf{M}_1$, $\mathbf{M}_2$ and $\mathbf{M}_3$ over $2N_f + 1$ frequencies, sorted as $\{0, 1, \ldots, N_f, -N_f, \ldots, -1\}$. This leads to:

$$\mathbf{M}_1 = \begin{pmatrix} \mathbf{O} & -g\mathbf{I} \\ \mathbf{G} & -\mathbf{C}_\omega \end{pmatrix}, \quad \mathbf{M}_2 = \begin{pmatrix} \mathbf{O} & -g\mathbf{I} \\ \mathbf{G} & -\mathbf{D}_{\perp 0}\mathbf{C}_\omega \end{pmatrix}, \quad \mathbf{M}_3 = \begin{pmatrix} \mathbf{O} & -g\mathbf{I} \\ \mathbf{G} & -\mathbf{D}_{LF}\mathbf{D}_{\perp 0}\mathbf{C}_\omega \end{pmatrix}, \tag{6.7}$$

with $\mathbf{G} = \mathrm{diag}(\{0, \tanh(d), \ldots, N_f \tanh(dN_f), N_f \tanh(dN_f), \ldots, \tanh(d)\})$ is the diagonal matrix corresponding to the Fourier multiplier operator $\mathcal{G}$, $\mathbf{I}$ the identity matrix, $\mathbf{O}$ the null matrix, $\mathbf{C}_\omega$ the matrix representing in Fourier space the application of the convolution product of the Fourier coefficients of the operator $\mathbf{1}_\omega$ onto a vector, $\mathbf{D}_{\perp 0}$ the diagonal matrix which removes mode 0 and $\mathbf{D}_{LF}$ the *low-frequency* projection matrix onto frequencies $\{-N_{init}, \ldots, N_{init}\}$. Note that, for simplicity reasons, we choose to set $\gamma = 1$. For a given matrix $\mathbf{M}_i$, $i \in \{1, 2, 3\}$ we solve the corresponding homogeneous linear ODE with *MATLAB* `ode45` solver. Numerical results are shown in Figure 6.1.

The non-convergence of the error equation (6.4) can therefore be observed, due to the obstruction coming from mode 0. Concerning the solution of the error equation (6.4), we can see the obstruction coming from the high frequencies, which prevents the desired convergence at low frequencies. Convergence is linear because, since the equation is discretized, we are in a finite-dimensional regime. But the rate of convergence is determined by the highest frequency represented by the grid, and not by the highest frequency which constitutes the initial condition. We can also see in Figure 6.1 (top right) and (bottom left) that although not existing in the initial conditions, high frequencies appear due to the indicator operator which mixes the frequencies, therefore supporting our theoretical results.

Finally, we can see that the solution to the error equation (6.5) converges at a linear rate determined by the highest frequency of the projector, which, as we know, is the same as in the initial condition. Figure 6.1 (bottom left) shows that this choice of observer does not create high frequencies.

6.3. Numerical study of the convergence rate. In this test, we focus on the rate of convergence of the observer. Once discretized in space, the problem falls within the framework of the section 5. We have linear convergence of the observer. This rate of convergence is therefore given by the largest real part of the eigenvalues of the observer matrix, *i.e.* the matrix $\mathbf{M}_2$ as presented in (6.7). We also know that this convergence rate depends on the highest frequency for a fixed observation interval ω. In Figure 6.2, we are therefore interested in the relationship between the number

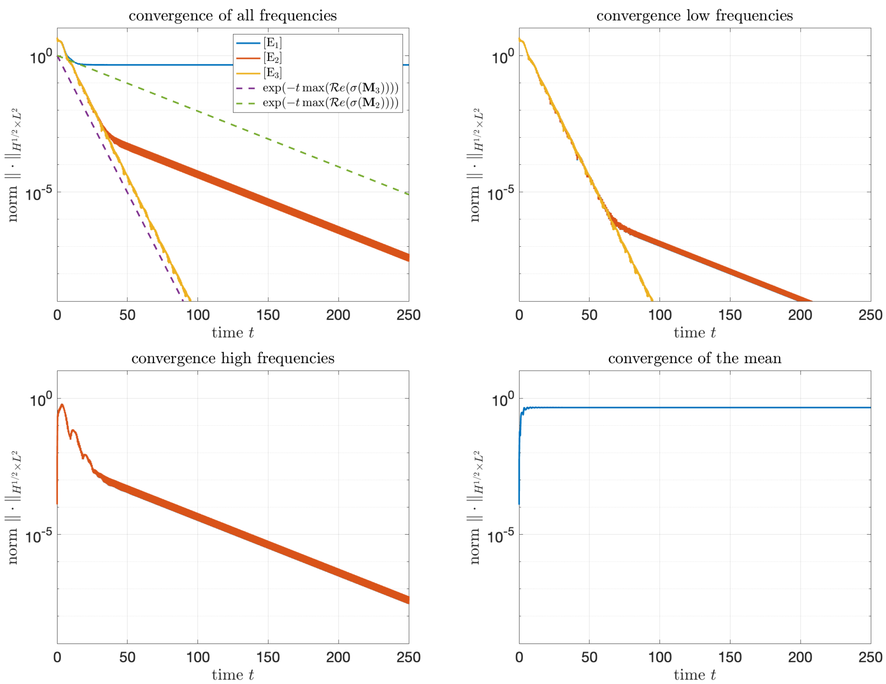

FIGURE 6.1. *Convergence of the error equation for the initial condition in (6.6). Top left: Convergence of the solution of [E_1], [E_2] and [E_3], with the theoretical rate of convergence found after an eigenvalue analysis of matrices $\mathbf{M}_2$ and $\mathbf{M}_3$. Top right: Same as top left, where the solutions have been projected onto the low frequencies, i.e., $\{-N_{init}, \dots, N_{init}\}$. Bottom left: Same as top left, where the solutions have been projected onto the high frequencies, i.e., $\{-N_f, \dots, N_f\} \backslash \{-N_{init}, \dots, N_{init}\}$. Bottom right: Same as top left, where the solutions have been projected onto the frequency* 0.

of frequencies represented and the rate of convergence. For increasing values of N_f, an increasingly large matrix $\mathbf{M}_2$ is constructed and its eigenvalue of largest real part is then extracted.

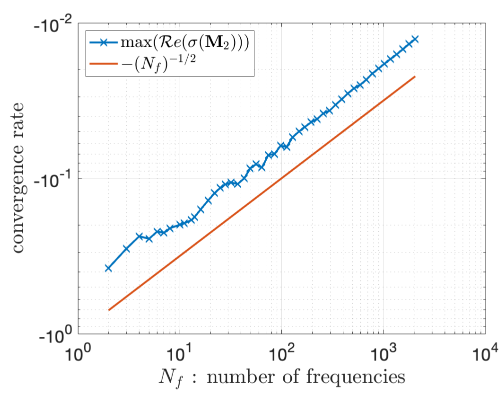

FIGURE 6.2. *Convergence factor* α *as in* $\|(\phi_{er}, \eta_{er})(t)\| \approx \exp(-\alpha t)$ *as function of the number of frequencies* N_f *reprensented.*

As can be seen in Figure 6.2, we therefore observe a linear convergence of the error at rate $(N_f)^{-1/2}$. Recall that theoretically, by Theorem 5.2, we have found that the convergence rate is at least of rate $(N_f)^{-2}$. Hence, it seems likely that our theoretical result is not optimal.

6.4. Application to wave field reconstruction. In this section, we focus on applying a Luenberger observer to a wave field in open sea, within a simplified but still relevant framework. These data are generated over a basin of length L.

$$\eta(t,x) = \mathrm{Re}\left\{\sum_{n=1}^{N} A_n \exp(i(|k_n|x - \omega_n t + \lambda_n))\right\} \tag{6.8}$$

where A_n are wave amplitudes of $N = 2048$ different individual waves calculated from a JONSWAP spectrum [16] with a peak period of 10 seconds, and a significant height of 3 meters. We then choose $L = 64 l_p$ where l_p is the peak wavelength. We then have $k_n = \frac{n2\pi}{L}$, and $\omega_n = \sqrt{g|k_n|\tanh(d|k_n|)}$, and λ_n are random phase shifts drawn on $[0, 2\pi[$.
We then aim to set up an observer on the interval $\mathit{\Omega} = [0, L/4[$, an interval divided into two, with an observation region $\widetilde{\mathit{\Omega}} = [0, L/8[$ and a prediction region $\mathit{\Omega}\backslash\widetilde{\mathit{\Omega}} = [L/8, L/4[$ as schematized in Figure 6.3. We therefore simulate a situation where we observe a wave field over an interval of size $8l_p$, and where we reconstruct this wave field over an interval twice as large, with the aim of predicting it over a region where we have no information. $\mathit{\Omega}$ is then discretized with a grid of $N_{\mathit{\Omega}} = 256$ points (we therefore have $N_{\widetilde{\mathit{\Omega}}} = N_{\mathit{\Omega}\backslash\widetilde{\mathit{\Omega}}} = 128$). We then solve the following observer equation on

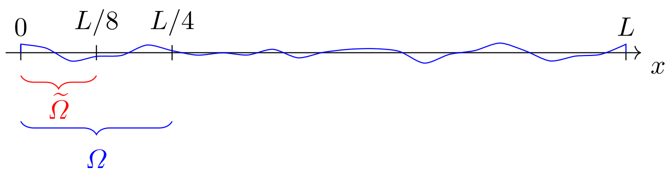

FIGURE 6.3. *Setting for the reconstruction of a synthetic wave field.*

$\mathit{\Omega} \times [0, T_{\mathrm{end}}]$:

$$\begin{cases} \partial_t \eta_o(x_l,t) &= -g\phi_o(x_l,t), \\ \partial_t \phi_o(x_l,t) &= \mathcal{G}(\eta_o(x_l,t)) + \gamma \mathit{\Pi}_{\perp 0} \mathbf{1}_{\widetilde{\mathit{\Omega}}}(\eta(x_l,t) - \eta_o(x_l,t)), \\ \eta_o(x_l,0) &= \mathbf{1}_{\widetilde{\mathit{\Omega}}}\eta(x_l,t), \\ \phi_o(x_l,0) &= 0. \end{cases} \tag{6.9}$$

The theoretical results given in section 5 no longer hold for two reasons. First, the η wave field is not periodic on $\mathit{\Omega}$. Second is that the discretization of $\mathit{\Omega}$ is coarser than that used to generate η synthetically. As explained in subsection 6.1, this second reason leads to aliasing, preventing us from achieving the linear convergence described in section 5. However, as long as the spectrum support of η is largely covered by the discretization grid of $\mathit{\Omega}$, we expect qualitative results. A prior statistical understanding of the spectrum of an open ocean wave field is therefore necessary, and this is why operations such as JONSWAP have been performed.

To validate our results, we use a different metric from the one used so far, called SSP, (*Surface Similarity Parameter*), which is used in the hydrodynamics community

[29, 19, 9]. It is defined as follows, for two signals f_1 and f_2:

$$\mathrm{SSP}(t) = \frac{\left(\sum_n |c_n(f_1) - c_n(f_2)|^2\right)^{1/2}}{\left(\sum_n |c_n(f_1)|^2\right)^{1/2} + \left(\sum_n |c_n(f_2)|^2\right)^{1/2}}. \tag{6.10}$$

The SSP has values in the range $[0, 1]$, where 0 corresponds to a perfect match and 1 corresponds to a perfect mismatch between the two signals.

Solving equation (6.9) with $\gamma = 0.2$ gives the results shown in Figure 6.4. Here, for a fixed time t, we compare the SSP score between the η function of the synthetic wave field evaluated at the grid points in Ω and the solution of (6.9). The corresponding snapshots are shown in Figure 6.5. The choice of $\gamma = 0.2$ is explained later.

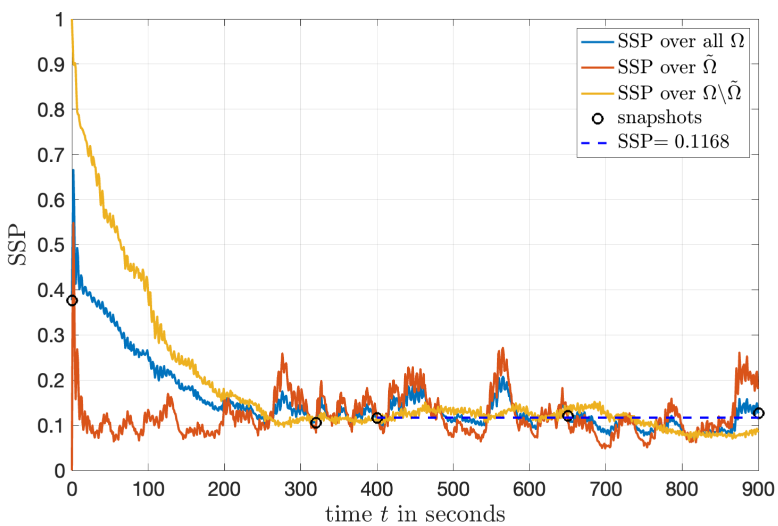

FIGURE 6.4. *SSP over time. Blue curve is the SSP on Ω, red curve is the SSP on $\widetilde{\Omega}$, yellow curve is the SSP on $\Omega\backslash\widetilde{\Omega}$, blue dotted curve is the mean value of the SSP on Ω over time interval* $[400, 900]$.

In Figure 6.4, we can see that the observer takes some time to reconstruct the whole Ω interval (around 400 seconds of simulation) before converging around an average SSP of 0.12. The snapshots in Figure 6.5 show a good reconstruction of the surface over Ω from $t = 400$ seconds. We are then interested in the impact of the gain constant γ on the observer, its convergence rate, and its average SSP once the first 400 seconds of simulation have elapsed. The results are shown in Figure 6.6. Figure 6.6 shows that, depending on the value chosen for the gain constant γ, the average SSP varies, and varies differently if we look at the whole simulation interval, only the observed one or only the reconstructed one. The results shown in Figure 6.4 and Figure 6.5 are therefore those with $\gamma = 0.2$ which equalize the SSP over the observation interval and the reconstruction interval, but we note that we can obtain better results over one of these intervals individually if we choose another value of γ.

REFERENCES

[1] T. Alazard, P. Baldi, and D. Han-Kwan. Control of water waves. *Journal of the European Mathematical Society*, 20, 01 2015.

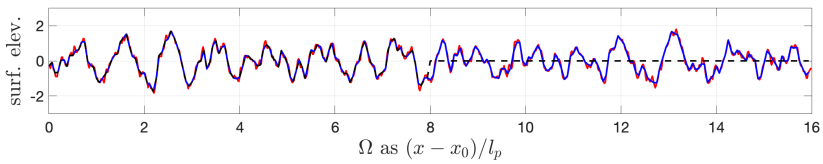

(a) solution at time $t = 0$

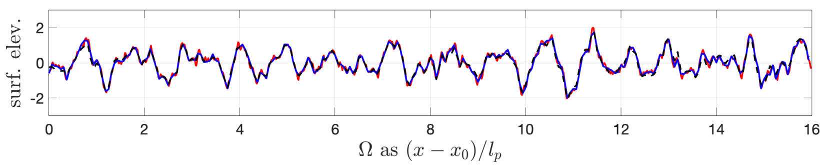

(b) solution at time $t = 320$

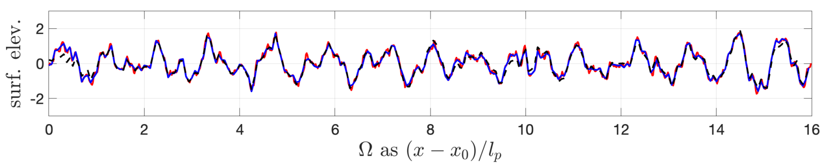

(c) solution at time $t = 400$

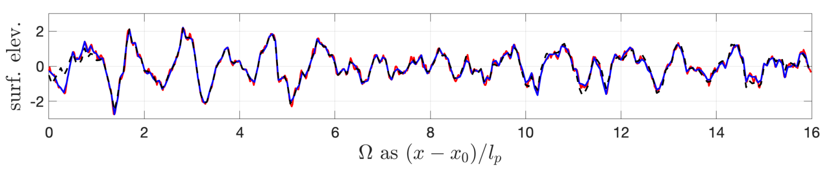

(d) solution at time $t = 650$

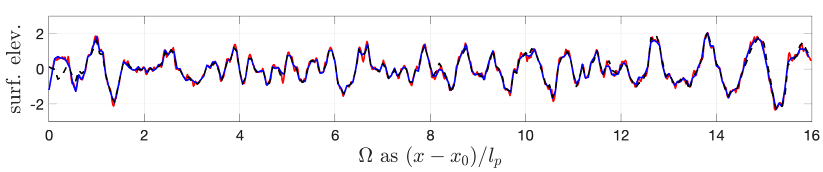

(e) solution at time $t = 900$

FIGURE 6.5. *Snapshots of the surface over Ω at different timesteps. Red curve is the full synthetic solution η on a fine grid, blue curve is the synthetic solution η on the grid used for the observer, black dotted curve is the reconstructed surface η.*

[2] J. Angel, J. Behrens, S. Götschel, M. Hollm, D. Ruprecht, and R. Seifried. Bathymetry reconstruction from experimental data using pde-constrained optimisation. *Computers & Fluids*, 278:106321, June 2024.

[3] A. Borichev and Y. Tomilov. Optimal polynomial decay of functions and operator semigroups. *Math. Ann.*, 347(2):455–478, 2010.

[4] L. Brivadis, V. Andrieu, U. Serres, and J.-P. Gauthier. Luenberger observers for infinite-dimensional systems, back and forth nudging, and application to a crystallization process. *SIAM J. Control Optim.*, 59(2):857–886, 2021.

[5] R. Chill, L. Paunonen, D. Seifert, R. Stahn, and Y. Tomilov. Nonuniform stability of damped contraction semigroups. *Anal. PDE*, 16(5):1089–1132, 2023.

[6] R. G. Dean and R. A. Dalrymple. *Water Wave Mechanics for Engineers and Scientists*. World

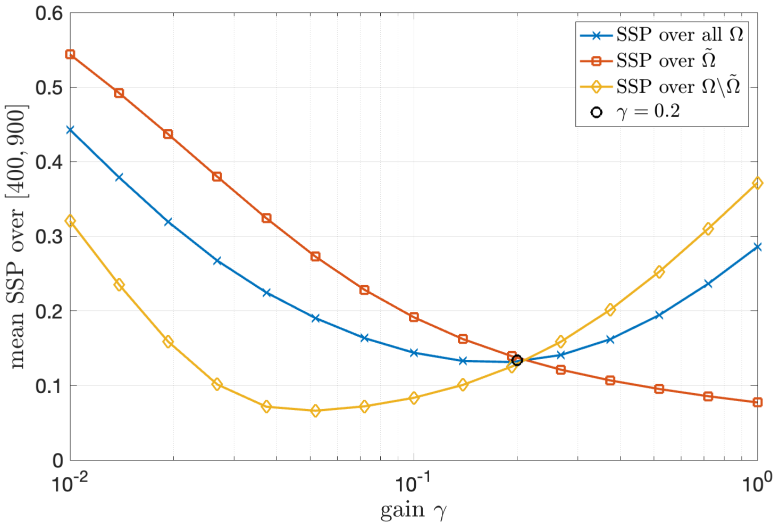

FIGURE 6.6. *mean SSP over* $[400, 900]$ *as a function of gain* γ*. Blue curve is the SSP on* Ω*, red curve is the SSP on* $\widetilde{\Omega}$*, yellow curve is the SSP on* $\Omega\backslash\widetilde{\Omega}$*.*

Scientific, 1991.

[7] N. Desmars. *Reconstruction et prédiction en temps réel de champs de vagues par télédétection optique*. PhD thesis, Ecole Centrale de Nantes, 2020.

[8] N. Desmars, F. Bonnefoy, S. Grilli, G. Ducrozet, Y. Perignon, C.-A. Guérin, and P. Ferrant. Experimental and numerical assessment of deterministic nonlinear ocean waves prediction algorithms using non-uniformly sampled wave gauges. *Ocean Engineering*, 212:107659, 2020.

[9] N. Desmars, M. Hartmann, J. Behrendt, N. Hoffmann, and M. Klein. Nonlinear deterministic reconstruction and prediction of remotely measured ocean surface waves. *Journal of Fluid Mechanics*, 975:A8, 2023.

[10] N. Desmars, M. Hartmann, J. Behrendt, M. Klein, and N. Hoffmann. Reconstruction of Ocean Surfaces From Randomly Distributed Measurements Using a Grid-Based Method. In *Volume 6: Ocean Engineering*, International Conference on Offshore Mechanics and Arctic Engineering, page V006T06A059, 06 2021.

[11] V. Duchêne. *Many Models for Water Waves*. Habilitation à diriger des recherches, Université de Rennes 1, July 2021.

[12] S. Ehlers, N. A. Wagner, A. Scherzl, M. Klein, N. Hoffmann, and M. Stender. Data assimilation and parameter identification for water waves using the nonlinear schrödinger equation and physics-informed neural networks, 2024.

[13] K.-J. Engel and R. Nagel. *One-parameter semigroups for linear evolution equations*, volume 194 of *Graduate Texts in Mathematics*. Springer-Verlag, New York, 2000.

[14] L. Gagnon, A. Hayat, S. Xiang, and C. Zhang. Fredholm backstepping for critical operators and application to rapid stabilization for the linearized water waves, 2022.

[15] G. Haine. Recovering the observable part of the initial data of an infinite-dimensional linear system with skew-adjoint generator. *Math. Control Signals Systems*, 26(3):435–462, 2014.

[16] K. Hasselmann, T. Barnet, E. Bouws, H. Carlson, D. Cartwright, K. Enke, J. Ewing, H. Gienapp, D. Hasselmann, P. Krusemann, A. Meerburg, P. Müller, D. Olbers, K. Richter, W. Seil, and H. Walden. Measurements of wind-wave growth and swell decay during the joint north sea wave project (jonswap). *Deutsche Hydrographische Zeitschrift, Reihe A*, 8(12):1–95, 1973.

[17] T. M. Inc. Matlab version: 24.1.0.2628055 (r2024a) update 4, 2024.

[18] N. K. R. Kevlahan and R. A. Khan. Convergence analysis of a variational data assimilation scheme for bathymetry detection from surface wave observations, 2020.

[19] M. Klein, M. Dudek, G. F. Clauss, S. Ehlers, J. Behrendt, N. Hoffmann, and M. Onorato. On the deterministic prediction of water waves. *Fluids*, 5(9), 2020.

[20] A. Koenig. Lack of null-controllability for the fractional heat equation and related equations.

SIAM J. Control Optim., 58(6):3130–3160, 2020.

[21] A. Koenig and P. Lissy. Null-controllability of underactuated linear parabolic-transport systems with constant coefficients, 2024.

[22] J. Kusters, K. Cockrell, B. Connell, J. Rudzinsky, and V. Vinciullo. Futurewaves™: A real-time ship motion forecasting system employing advanced wave-sensing radar. In *OCEANS 2016 MTS/IEEE Monterey*, pages 1–9, 2016.

[23] D. Lannes. *The Water Waves Problem: Mathematical Analysis and Asymptotics*. Mathematical surveys and monographs. American Mathematical Society, 2013.

[24] K. Liu. Locally distributed control and damping for the conservative systems. *SIAM J. Control Optim.*, 35(5):1574–1590, 1997.

[25] D. P. Mitchell and A. N. Netravali. Reconstruction filters in computer-graphics. In *Proceedings of the 15th Annual Conference on Computer Graphics and Interactive Techniques*, SIGGRAPH '88, page 221–228, New York, NY, USA, 1988. Association for Computing Machinery.

[26] H. Monajemi. *Data Assimilation for Shallow Water Waves: Application to Flood Forecasting*. PhD thesis, Carleton University, 08 2009.

[27] P. Naaijen, K. Trulsen, and E. Blondel-Couprie. Limits to the extent of the spatio-temporal domain for deterministic wave prediction. *International Shipbuilding Progress*, 61(3-4):203–223, 2014.

[28] A. Pazy. *Semigroups of linear operators and applications to partial differential equations*, volume 44 of *Applied Mathematical Sciences*. Springer-Verlag, New York, 1983.

[29] M. Perlin and M. D. Bustamante. A robust quantitative comparison criterion of two signals based on the sobolev norm of their difference. *Journal of Engineering Mathematics*, 101(1):115–124, 2016.

[30] A. B. Rabinovich. Twenty-seven years of progress in the science of meteorological tsunamis following the 1992 daytona beach event. *Pure and Applied Geophysics*, 177(3):1193–1230, 2020.

[31] J. Royer. *The Damped Wave Equation and other Evolution Problems involving Non-selfadjoint Operators*. Habilitation à diriger des recherches, Université Paul Sabatier (Toulouse 3), Dec. 2022.

[32] M. Slemrod. A note on complete controllability and stabilizability for linear control systems in Hilbert space. *SIAM J. Control*, 12:500–508, 1974.

[33] P. Su, M. Tucsnak, and G. Weiss. Stabilizability properties of a linearized water waves system. *Systems & Control Letters*, 139:104672, 2020.

[34] M. Tucsnak and G. Weiss. *Observation and control for operator semigroups*. Birkhäuser Advanced Texts: Basler Lehrbüche. Birkhäuser Verlag, Basel, 2009.

[35] G. Wang, J. Zhang, Y. Ma, Q. Zhang, Z. Li, and Y. Pan. Phase-resolved ocean wave forecast with simultaneous current estimation through data assimilation. *Journal of Fluid Mechanics*, 949, Sept. 2022.

[36] Y. Yu, H.-L. Pei, and C.-Z. Xu. Estimation of velocity potential of water waves using a luenberger-like observer. *Science China Information Sciences*, 63, 12 2020.